HIGH ORDER LES OF THE TURBULENT 'AHMED BODY' WAKE FLOW

***M. Minguez*[1,2], *R. Pasquetti*[2] *and E. Serre*[1]**

[1] ***Lab. MSNM-GP, UMR CNRS 6181, Technopôle de Château Gombert, 13451 Marseille***
[2] ***Lab. J.A. Dieudonné, UMR CNRS 6621, Parc Valrose, 06108 Nice***

richard.pasquetti@unice.fr

Abstract

The simulation of the turbulent wake of a classical car model, the Ahmed body, is addressed. The numerical solver makes use of a multi-domain Fourier - Chebyshev approximation. The LES capability is implemented through the use a spectral vanishing viscosity technique. Comparisons are provided between results obtained for two different values of the Reynolds number, $Re = 768000$ and $Re = 8322$.

1 Introduction

The Ahmed body wake flow is a well known test-case to check the capability of Reynolds Averaged Navier-Stokes (RANS) or Large-Eddy Simulation (LES) approaches, see e.g. Manceau et al. (2000). This simple car model is essentially parallelepipedic and exhibit a slant face at the rear, see e.g. Hinterberger et al. (2004) for a precise description. As first shown in Ahmed and Ram (1984), depending on the inclination of the slant different flows may be obtained: For a slant angle greater than about 30^0 one has a large detachment of the flow whereas for smaller angles the flow reattaches on the slant. These different behaviors of the flow are associated to a drag crisis, with a sudden decrease of the drag coefficient at the critical $\alpha = 30^0$ value. Generally, RANS and LES studies focus on the subcritical and supercritical cases, $\alpha = 25^0$ and $\alpha = 35^0$, respectively, at the Reynolds number $Re = Uh/\nu = 768000$, where h is the height of the vehicle, U the upstream velocity and ν the kinematic viscosity. If RANS approaches provide good results for the supercritical case, results are poor in the subcritical situation, see Guilmineau (2007). LES approaches have provided some encouraging results in this latter case, but none of them are fully satisfactory with respect to the experimental data, see e.g. Howard and Pourquie (2002), Hinterberger et al. (2004), Fares (2006)... This is why the Ahmed wake flow constitutes a valuable and challenging benchmark for RANS or LES methodologies.

Here we are interested in a LES computation of the subcritical $\alpha = 25^0$ case, using a high order spectral method. The LES capability is implemented thanks to a Spectral Vanishing Viscosity (SVV) method and the bluff body is modeled through the use of a 'pseudo-penalization' technique. Moreover, computations have been carried out for the usual Reynolds $Re = 768000$ but also for the much smaller value $Re = 8322$, in connection with the experiment of Gillieron and Chometon (1999), with the aim to check the sensitivity of the flow to this control parameter. The paper shows three parts: The numerical modeling is first described, computational details are then given and some numerical results are finally provided.

2 Numerical Modeling

The modeling is based on the incompressible Navier-Stokes (NS) equations stabilized with a SVV term (SVV-LES approach). The geometry is channel like. At the initial time the fluid is a rest. Free slip boundary conditions are considered at the upper part of the channel. No-slip conditions are enforced at the walls, i.e. at the ground and at the obstacle. A boundary layer profile is enforced at the inlet. At the outlet one uses a convective type soft outflow boundary condition.

The numerical solver is based on a multidomain Chebyshev - Fourier method : A domain decomposition is used in the elongated direction of the flow, in each subdomain one uses a standard collocation Chebyshev method in the x-streamwise and y-vertical directions, and Fourier expansions in the z-spanwise direction which is assumed homogeneous. In time we use a 3 steps method: (i) an explicit transport step, based on an OIF (Operator Integration Factor) semi-Lagrangian method and a RK4 scheme to handle the advection term, (ii) an implicit diffusion step and (iii) a projection step, to get a divergence free velocity field. The time scheme is globally second order accurate. Details may be found in Cousin and Pasquetti (2004).

A volume penalization method is used to model the obstacle. However, no penalization term is explicitly introduced in the momentum equation. This is implicitly done through the time discretized equation, as suggested in Pasquetti et al. (2007a). With χ for the characteristic function of the obstacle and $C \gg 1$ a constant coefficient, the standard volume penalization

method makes use of the penalized NS equations :

$$D_t \boldsymbol{u} = -\nabla p + \nu \Delta \boldsymbol{u} - C\chi \boldsymbol{u} \quad (1)$$

$$\nabla \cdot \boldsymbol{u} = 0 \quad (2)$$

with t for the time, $\boldsymbol{u}$ for the velocity, p for a pressure term and where D_t is the material derivative. In dimensionless form, ν is the inverse of the Reynolds number. Clearly, outside the obstacle we recover the NS equations, whereas inside if C is infinite then $\boldsymbol{u} = 0$.

For the pseudo-penalization method we restart from the NS equations and assume that the linear diffusive term is treated implicitly and the non-linear convective term explicitly. Then the following semi-discrete equations must be solved at each time-step:

$$\nu \Delta \boldsymbol{u}^{n+1} - \frac{\alpha}{\tau}\boldsymbol{u}^{n+1} - \nabla p^{n+1} = \boldsymbol{f}^{n+1} \quad (3)$$

$$\nabla \cdot \boldsymbol{u}^{n+1} = 0 \quad (4)$$

where n is the time index, τ the time-step and α a scheme dependent coefficient ($\alpha = 3/2$ for a second-order backward finite difference scheme). The pair $(\boldsymbol{u}^n, p^n)$ is the numerical approximation of $(\boldsymbol{u}, p)$ at time t_n and $\boldsymbol{f}^{n+1}$ is an easily identifiable source term, which also depends on the time scheme. With again χ for the characteristic function of the obstacle, the pseudo-penalization method consists of solving:

$$\nu \Delta \boldsymbol{u}^{n+1} - \frac{\alpha}{\tau}\boldsymbol{u}^{n+1} - \nabla p^{n+1} = (1-\bar{\chi})\boldsymbol{f}^{n+1} \quad (5)$$

$$\nabla \cdot \boldsymbol{u}^{n+1} = 0 \quad (6)$$

where $\bar{\chi}$ is a regularized characteristic function, in practice obtained from local averages of the function χ. Clearly, inside the obstacle $(\boldsymbol{u}^{n+1}, p^{n+1})$ solves the steady Stokes equations with a $O(1/\tau)$ penalization term. Then it appears that inside the obstacle the velocity approximately vanishes, i.e. is essentially $O(\tau) \ll 1$.

The LES capability is implemented through the use of a SVV technique. The SVV method was first developed to handle with spectral methods hyperbolic problems, typically the Burgers equation with initial data such as a shock develops. Basically, it consists of introducing some artificial viscosity in the high frequency range of the spectral approximation. This allows to stabilize the computation together with preserving the exponential rate of convergence of spectral methods. Using the SVV technique for LES was first suggested in Karamanos and Karniadakis (2000) (see also Kirby and Karniadakis (2002)). For us we have largely developed the SVV-LES approach in the frame of variational or collocation methods, see Xu and Pasquetti (2004) and Pasquetti (2006a), and also when cylindrical geometries are concerned, see Pasquetti et al. (2007b) and Severac and Serre (2007). Note however that extending the SVV method from 1D Burgers to 3D Navier-Stokes is not trivial and it is of interest to observe that at the end the algorithms differ ! In the SVV-LES version of the solver we consider the following stabilized momentum equation:

$$D_t \boldsymbol{u} = -\nabla p + \nu \nabla \cdot S_N(\nabla \boldsymbol{u}) \quad (7)$$

with S_N a diagonal operator which depends on the space discretization parameter N:

$$S_N \equiv diag\{1 + \frac{\epsilon_{N_i}}{\nu} Q^i_{N_i}\}_{i=1,\cdots,3} \quad (8)$$

where the subscript i denotes the i-direction (we use here x_i for x, y and z) and where appear the amplitude coefficient and spectral viscosity operator, ϵ_N and Q_N in 1D, as introduced in the periodic case (Fourier approximation) in Tadmor (1989) and in the non-periodic case (Legendre approximation) in Maday et al. (1993). Note that Q_N is essentially characterized by a threshold frequency m_N upper which the SVV acts. Typically, $\epsilon_N = O(1/N)$ and $m_N = O(\sqrt{N})$.

For the Ahmed body problem we use mappings in the x-streamwise and y-crossflow directions. Since the polynomial approximation holds in the reference domain, say $\hat{\Omega}$, with the mapping $\boldsymbol{f} : \hat{\Omega} \rightarrow \Omega$, the operator S_N is defined as follows:

$$S_N(\nabla \boldsymbol{u}) \equiv S_N(\hat{\nabla}\hat{\boldsymbol{u}})\, G \quad (9)$$

where G is the Jacobian matrix of $\boldsymbol{f}^{-1}$ and $\hat{\boldsymbol{u}} = \boldsymbol{u} \circ \boldsymbol{f}$.

The practical implementation of the operator S_N is based on the introduction of SVV modified differentiation matrices. From the previous definition of S_N we indeed have:

$$[\nabla \cdot S_N(\nabla \boldsymbol{u})]_i = \sum_j \partial_j(\tilde{\partial}_j \boldsymbol{u}_i) \quad (10)$$

where $\tilde{\partial}_j = (1 + \nu^{-1}\epsilon_{N_j} Q^j_{N_j})\, \partial_j$.

As well known, as soon as the Reynolds number is really high, as it is for the Ahmed body flow at $Re = 768000$, the boundary layers cannot be resolved properly by the mesh. This has motivated a lot of researches during the three last decades on Near Wall Modeling (NWM), see e.g. Piomelli and Balaras (2002). The problem is especially difficult when the flow shows large detachments. Several approaches have been suggested, based on the boundary layer equations or requiring to resolve joined equations, see Wang and Moin (2002), patching techniques, DES (Detached Eddy Simulation) methods, see Menter and Kuntz (2003)... Such approaches have essentially been developed for finite volume approximations and it is not straightforward to implement them in a spectral solver and when using a penalization type method.

The results presented in this paper have been obtained with a cruder approach but which has allowed significant improvements : (i) the characteristic function of the obstacle is not smoothed and (ii) the control parameters of the SVV technique, ϵ_N and m_N, are relaxed in the Near Wall region. This may be formulated

as:

$$D_t \boldsymbol{u} = -\nabla p + \nu \nabla \cdot S_N(\nabla \boldsymbol{u}) - C\chi \boldsymbol{u} + \boldsymbol{f}_{BL} \quad (11)$$

with BL for Boundary Layer and where:

$$\boldsymbol{f}_{BL} = \chi_{BL} \nu \nabla \cdot (S_N^{BL}(\nabla \boldsymbol{u}) - S_N(\nabla \boldsymbol{u})). \quad (12)$$

In this expression χ_{BL} is a second characteristic function used to localize the NW adjustment, whereas the non-regularized function χ is used to model the bluff body via the pseudo-penalization technique. The operator S_N^{BL} is defined like S_N but makes use of a smaller value of ϵ_N and / or a greater value of m_N. In practice, we have only increased the value of m_N within the NW region.

3 Computational details

Computations were carried out in the domain $(-7.25, 7.25) \times (0, 3.47) \times (-2.35, 2.35)$. The height of the car model is used as reference length and the rear part is located at $x = 0$. The computational domain is partitioned in 8 subdomains, the code is parallelized and each subdomain is associated to a (vectorial) processor. In each one the discretization is $41 \times 191 \times 340$, obtained with Chebyshev polynomials of degrees $N_x = 40$ and $N_y = 190$ and trigonometric polynomials of degree $N_z = 170$. Since Gauss-Lobatto-Chebyshev points naturally accumulate at the end-points, subdomains interfaces have been located at the front and rear part of the Ahmed body. In the vertical direction, non-linear mappings are used to accumulate grid-points on the upper part of the bluff body. The mesh, see Fig. 1, makes use of about 21 millions of grid-points.

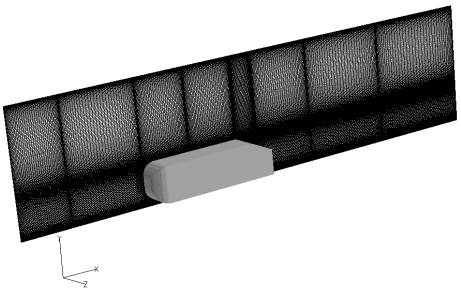

Figure 1: Visualization of the mesh.

Starting from the fluid at rest, a computation was first carried out on a rough mesh (discretization is roughly divided by 2 in each direction) till a turbulent flow is well established, say at the dimensionless time $t = 100$ (reference time, h/U). Then, the solution was interpolated on a fine mesh and the simulation was continued till $t = 160$. Statistics were only computed during the last 40 time units of the simulation, in order to avoid any pollution coming from the coarse mesh computation. The dimensionless time-step was equal to $\tau = 2.10^{-3}$ and the CPU time to $9\,s$ for one time-step, *i.e.* approximately $9.510^{-8}s$ per iteration and degree of freedom on the NEC SX8 computer of the IDRIS center.

The SVV stabilization is governed by the threshold frequency m_N and the SVV amplitude ϵ_N. Independently of the spatial (x, y, z) direction, outside the boundary layer we have used $m_N = \sqrt{N}$ and $\varepsilon_N = 1/N$. Within the boundary layer, we have used anisotropic values, i.e. $m_N = \{2\sqrt{N_x}, 5\sqrt{N_y}, 4\sqrt{N_z}\}$ and again $\varepsilon_N = 1/N$.

4 Numerical results

Results obtained at the reference Reynolds number $Re = 768000$ and comparisons with results obtained at $Re = 8322$ are provided. Same meshes and time-steps have been used in the two cases and the values of the SVV control parameters are the same, both inside and outside the boundary layers (see previous Section). However, for computational cost reasons we only used 12 time units to get the statistical results at the lower Reynolds number. As described hereafter, the topology of the two flows are in fact close, showing that the flow is not very sensitive to the Reynolds number. More details may be found in Minguez et al. (2008).

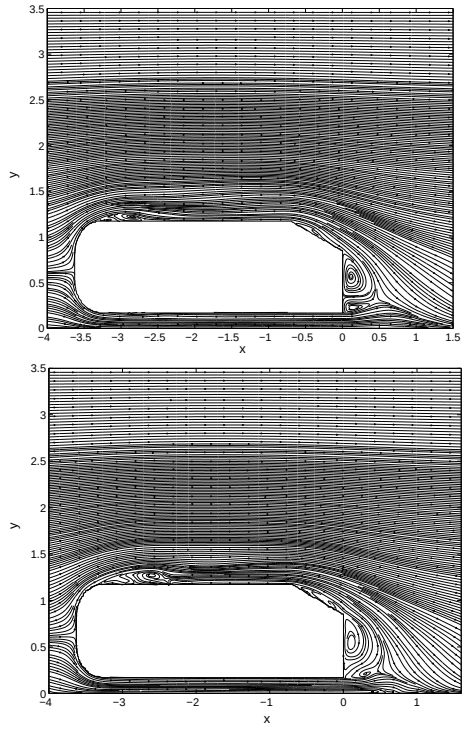

Figure 2: Mean streamlines in the median plane $z = 0$ for $Re = 768000$ (up) and $Re = 8322$ (bottom).

In Fig. 2 we compare isolines of the mean stream-

function in the vertical median plane $z = 0$. One clearly observes three recirculation zones, on the upper part of the body, over the slant and behind the obstacle. Moreover, recirculation bubbles similar to the one in the upper part occur at the lateral walls. Despite similar, these recirculation zones appear larger, i.e. longer and thicker, at the lower Reynolds number. Behind the obstacle the topology is slightly different : The recirculation zone shows two contra-rotating recirculation bubbles and one observes that the lower one is less pronounced at $Re = 8322$, which probably results from a thicker boundary layer developing under the body. One should mention that no recirculation regions in the front part are described in the experiments at $Re = 768000$ of Lienhart et al. (2000). At this point it of interest to mention the work of Krajnovic and Davidson (2004, 2005), where the Ahmed body flow at the Reynolds number $Re = 200000$ is addressed. The authors report the occurrence of a recirculation bubble on the roof, as well as similar ones of the lateral sides, discuss the importance of these recirculation zones on the downstream development of the flow, but cannot conclude if at the higher Reynolds number $Re = 768000$ such recirculation bubbles are still present.

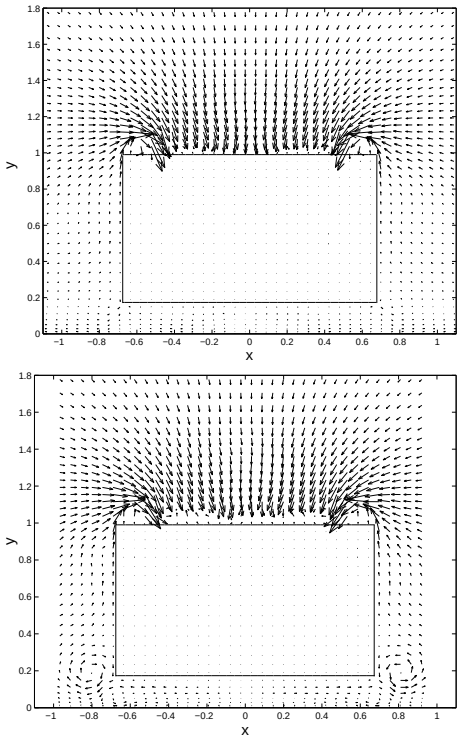

Figure 3: Transverse velocity field at $x = -0.31$ for $Re = 768000$ (up) and $Re = 8322$ (bottom).

In Fig. 3 are shown velocity fields in the plane $x = -0.31$ for the two values of the Reynolds number. Clearly, the cone like trailing vortices which escape from the edge of the slant are similar. Note that for the reference Reynolds $Re = 768000$, comparisons with the experiments are satisfactory, see Minguez et al. (2007). However, at the low Re one clearly observes additional trailing vortices close to the ground, on each side of the Ahmed body, and contrarily to our results such trailing vortices are still present in the experiments of Lienhart et al. (2000).

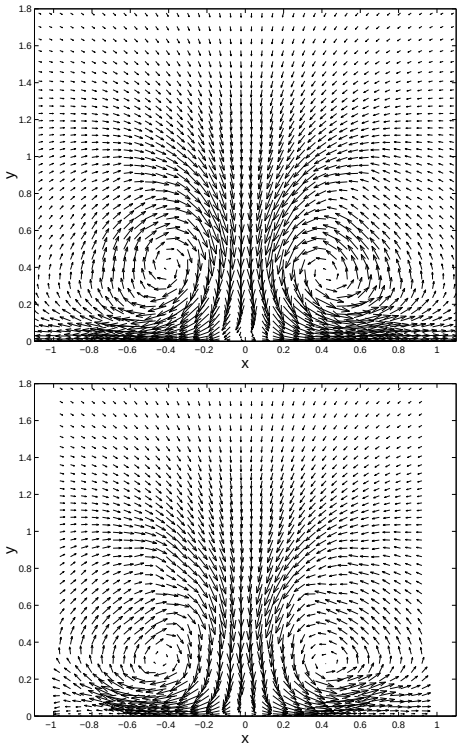

Figure 4: Transverse velocity field at $x = 1.34$ for $Re = 768000$ (up) and $Re = 8322$ (bottom).

A similar visualization downstream, at $x = 1.34$, is shown in Fig. 4. For the lower Reynolds number the vortices appear (i) slightly more distant and (ii) are located lower.

We compare in Fig. 5 mean streamwise velocity and turbulent kinetic energy profiles. Under the body one observes that the flow is nearly laminar for the low Re simulation : a parabolic like profile is obtained and the turbulent kinetic energy is close to 0. This is not very surprising, since the local Reynolds number based on the distance from the body to the ground equals 1445. Over the slant, one recovers the conclusion inferred by the mean streamlines that the reattachment is delayed.

For the higher Re comparisons with the experiments of Lienhart et al. (2000) are provided in Minguez et al. (2007), but to be self contained we present in Fig. 6 such comparisons, for the mean streamwise velocity and for the turbulent kinetic energy. We also point out the influence of the NW correction. Even if the SVV-LES profiles compare rather well with the experimental data, one observes at the beginning of the slant a deficit of streamwise veloc-

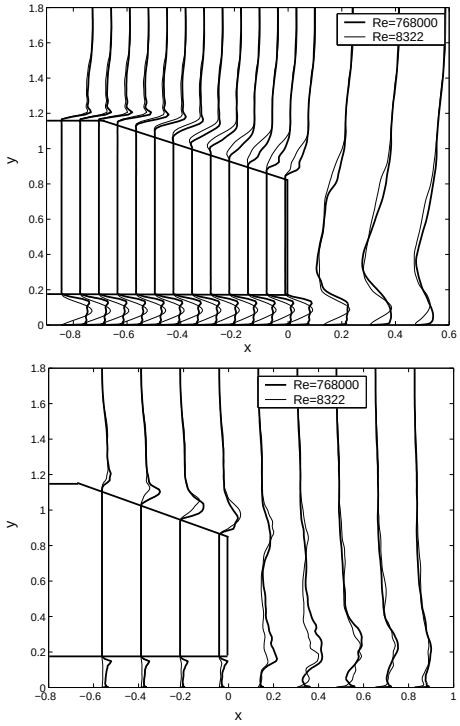

Figure 5: Mean streamwise velocity (up) and turbulent kinetic energy at $z = 0$ for $Re = 8322$ and $Re = 768000$.

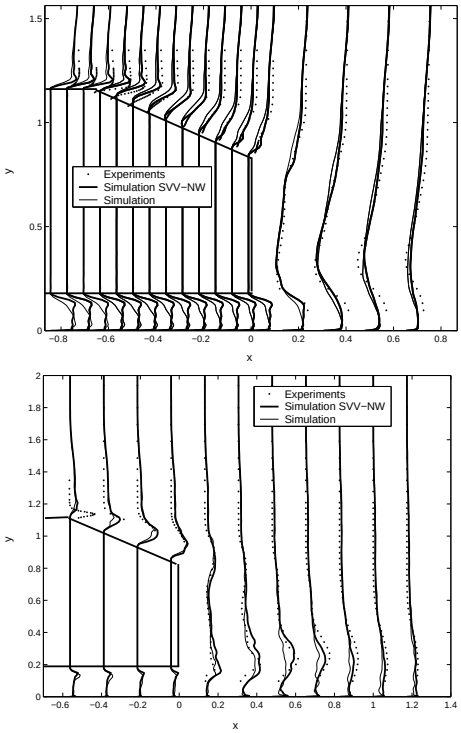

Figure 6: Mean streamwise velocity (up) and turbulent kinetic energy at $z = 0$ for $Re = 768000$. Comparisons with the experiment of Lienhart et al. (2000). Numerical results with (SVV-NW) and without relaxation of SVV in near wall region.

ity associated to an overestimation of the turbulent kinetic. The phenomenon is in fact confined in the median region, say for $-0.5 < z < 0.5$ and develops from the front part of the body, downstream of the recirculation bubble localized on the upper part, see Fig. 2. Such a recirculation bubble is not obtained in the simulations of Hinterberger et al. (2004) and it is not not known if it was observed in the experiments of Lienhart et al. (2000). As previously discussed, such recirculation regions are however mentioned in Krajnovic and Davidson (2004, 2005) where the Ahmed body flow at the lower Reynolds number $Re = 200000$ is addressed.

Of course, the results obtained here at the lower value of the Reynolds number are certainly more reliable, since the SVV stabilization plays here a less important role. This may be visualized by computing the dissipation rate of the turbulent kinetic energy. In the frame of the present SVV-LES formulation it reads, see Pasquetti (2006b) :

$$\varepsilon \approx 2\nu(< S : \tilde{S} > - < S >:< \tilde{S} >) \,. \qquad (13)$$

In this expression S is the usual strain rate tensor and $\tilde{S}$ a similar tensor but computed with the SVV modified differentiation matrices :

$$S_{ij} = (\partial_i u_j + \partial_j u_i)/2 \,, \quad \tilde{S}_{ij} = (\tilde{\partial}_i u_j + \tilde{\partial}_j u_i)/2 \,. \qquad (14)$$

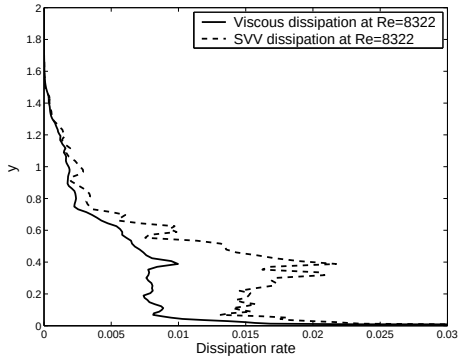

Figure 7: Dissipation rate and its viscous component at $x = 1.51, z = 0$.

In Fig. 7 we show the profile of ε in the vertical median plane at $x = 1.51$. The viscous part is also presented. As can be seen, the global (SVV) dissipation and its viscous part are roughly in a ratio 2. On the contrary, for $Re = 768000$ the SVV dissipation is two order of magnitude greater than its viscous part.

5 Conclusions

The basics of the SVV-LES approach used to compute the Ahmed body flow have been summarized : a spectral solver is used, the obstacle is modeled with a pseudo-penalization technique and the LES capability

is implemented thanks to the Spectral Vanishing Viscosity method. Our NW treatment is based on a relaxation of the SVV threshold frequency and the characteristic function of the obstacle is not smoothed.

Results have been presented for both the reference Reynolds number $Re = 768000$ and the much lower one, $Re = 8322$. Despite the similarity of the two flows, some differences were observed: The recirculation regions are larger at low Reynold and additional trailing vortices occur on the lateral parts. More details are provided in Minguez et al. (2008). For the high Reynolds flow we have outlined that the numerical results are in fairly agreement with the experiments, despite the fact that some discrepancies remain above the slant, probably associated to the occurrence of a recirculation zone in the front part of the car model.

Acknowledgments

The computations were done on the NEC-SX8 Computer of the IDRIS Computational Center (project 074055) and on the parallel computer of the SIGAMM Computational center at the OCA (Nice). The work was supported by the CNRS in the frame of the DFG-CNRS program “LES of complex flows”.

References

Ahmed, S.R. and Ramm, G. (1984), Some salient features of the time-averaged ground vehicle wake, SAE Technical Paper 840300.

Cousin, L. and Pasquetti, R. (2004), High-order methods for the simulation of transitional to turbulent wakes, *Advances in Scientific Computing and Applications*, Editors Y. Lu, W. Sun, T. Tang, Sciences Press Beijing/New York, 133-143.

Fares, E. (2006), Unsteady flow simulation of the Ahmed reference body using a lattice Boltzmann approach, *Computers & Fluids*, 35 (8-9), 940.

Gillieron, P. and Chometon, F. (1999), Modelling of stationary three-dimensional separated air flows around an Ahmed reference model, ESAIM Proc., 7, 173.

Guilmineau, E. (2007), Computational study of flow around a simplified car body, *J. Wind Eng. Ind. Aerodyn.*, doi:10.1016/j.jweia.2007.06.041.

Hinterberger, M., Garcia-Villalba, M. and Rodi, W. (2004), Large eddy simulation of flow around the Ahmed body, in Lectures Notes in Applied and Computational Mechanics / The aerodynamic of heavy vehicles: Trucks, Buses and Trains, R. Mc Callen, F. Browand, J. Ross (Eds), Springer Verlag, ISBN: 3-540-22088-7.

Howard, R.J.A. and Pourquie, M. (2002), Large eddy simulation of an Ahmed reference model, *J. of Turbulence*, 3.

Karamanos, G.S. and Karniadakis, G.E. (2000), A spectral vanishing viscosity method for large-eddy simulation, *J. Comput. Phys.*, 163, 22.

Kirby, R.M. and Karniadakis, G.E. (2002), Coarse resolution turbulence simulations with spectral vanishing viscosity - Large Eddy Simulation (SVV-LES), *J. Fluids Engineering*, 124 (4), 886-891.

Krajnovic, S. and Davidson, L. (2004), Large-eddy simulation of the flow around simplified car model, SAE Congress, SAE Paper No. 2004-01-0227, Détroit (USA).

Krajnovic, S. and Davidson, L. (2004), Large-eddy simulation of the flow around an Ahmed body, ASME HTFED04 Congress, Paper HT-FED2004-56325, Charlotte (USA).

Krajnovic, S. and Davidson, L. (2005), Flow around a simplified car, *J. of Fluids Engineering.*, 127, 907-918 and 919-928.

Lienhart, H., Stoots, C. and Becker, S. (2000), Flow and turbulence structures in the wake of a simplified car model (Ahmed Body). DGLR Fach Symp. der AG STAB, Stuttgart University, 15-17 Nov..

Maday, Y., Kaber, S.M.O. and Tadmor, E. (1993), Legendre pseudo-spectral viscosity method for nonlinear conservation laws, *SIAM J. Numer. Anal.*, 30 (2), 321-342.

Manceau, R. and Bonnet, J.P. (2000), ”10th joint ERCOFTAC (SIG-15)/IAHR/QNET-CFD Workshop on Refined Turbulence Modelling”, Poitiers.

Menter, F.R. and Kuntz, M. (2003), Development and application of a zonal DES turbulence model for CFX-5, CFX Internal Rep., Otterfing, Germany.

Minguez, M., Pasquetti, R. and Serre, E. (2007), Spectral vanishing viscosity stabilized LES of the Ahmed body turbulent wake, ICOSAHOM 07 Congress, Beijing, 18-22 juin 2007.

Minguez, M., Pasquetti, R. and Serre, E. (2007), Simulation des grandes échelles du sillage turbulent du corps d’Ahmed par une méthode de viscosité spectrale évanescente, 18ième Congrès Français de Mécanique, Grenoble, August 27 - 31 (proc. in CD).

Minguez, M., Pasquetti, R. and Serre, E. (2008), High-order LES of the flow over a simplified car model : effect of the viscosity, *Europ. J. of Comput. Mech.*, submitted.

Pasquetti, R. (2006a), Spectral vanishing viscosity method for large eddy simulation of turbulent flows, *J. Sci. Comp.*, 27 (1-3), 365-375, & ICOSAHOM 2004 Congress.

Pasquetti, R. (2006b), Spectral vanishing viscosity method for high-order LES: Computation of the dissipation rates, ECCOMAS CFD 2006, P. Wesseling, J. Onate, J. Périaux (Eds), Delft The Netherland (proc. on line).

Pasquetti, R., Bwemba, R. and Cousin, L. (2007a), A pseudo-penalization method for high Reynolds number unsteady flows, *Appl. Numer. Math.*, on line.

Pasquetti, R., Severac, E., Serre, E., Bontoux, P. and Schaefer, M. (2007b), From stratified wakes to rotor-stator flows by an SVV-LES method, *Theor. Comput. Fluid Dyn.*, on line.

Piomelli, U. and Balaras, E. (2002), Wall-layer models for large-eddy simulations, *Annu. Rev. Fluid Mech.*, 34, 349-374.

Severac, E. and Serre, E. (2007), A spectral vanishing viscosity for the LES of turbulent flows within rotating cavities, *J. Comput. Phys.*, 226, 1234-1255.

Tadmor, E. (1989), Convergence of spectral methods for nonlinear conservation laws, *SIAM J. Numer. Anal.*, 26 (1), 30-44.

Wang, M. and Moin, P. (2002), Dynamic wall modeling for large-eddy simulation of complex turbulent flow, *Phys. Fluids*, 14 (7), 2043-2051.

Xu, C.J. and Pasquetti, R. (2004), Stabilized spectral element computations of high-Reynolds number incompressible flows, *J. of Comp. Phys.*, 196 (2), 680-704.